

Could the width of the diphoton anomaly signal a three-body decay?

JÉRÉMY BERNON¹ AND CHRISTOPHER SMITH²

*Laboratoire de Physique Subatomique et de Cosmologie,
Université Grenoble-Alpes, CNRS/IN2P3, 53 avenue des Martyrs, 38026 Grenoble Cedex, France.*

Abstract

The recently observed diphoton anomaly at the LHC appears to suggest the presence of a rather broad resonance. In this note, it is pointed out that this broadness is not called for if the two photons are produced along with an extra state. Specifically, the diphoton invariant mass arising from various $A \rightarrow B\gamma\gamma$ processes, with A, B being scalars, fermions, or vectors, though peaked at a rather large value, would naturally be broad and could fit rather well the observed deviations. This interpretation has a number of advantages over the two-photon resonance hypothesis, for example with respect to the compatibility with the 8 TeV diphoton, dilepton or dijet searches, and opens many new routes for New Physics model construction.

¹ bernon@lpsc.in2p3.fr

² chsmith@lpsc.in2p3.fr

1 Introduction and set-up

Recently, a small deviation in the diphoton mass spectrum was announced by both ATLAS [1] and CMS [2] at a mass of around 750 GeV. While the statistical significance of this signal is still low, the simultaneous observation by both experiments lends some credence to the presence of a yet unknown resonance in this channel, and has led to an incredibly intense phenomenological activity (see Refs. [4] to [41]).

In this note, we want to point out that one feature of this $\gamma\gamma$ signal, namely its width, could be well explained if it arises from a three-body decay $A \rightarrow B\gamma\gamma$, with the mass splitting $M_A - M_B$ a bit higher than 750 GeV. The B particle would either be stable and escape undetected, or would be produced on-shell and would subsequently decay into some other invisible states.

Let us recall that the differential rate for the decay $A \rightarrow B\gamma\gamma$ depends only on the invariant mass of the two photons, $z \equiv m_{\gamma\gamma}^2/M_A^2$, or equivalently, on the B momentum $P_B \equiv |\mathbf{p}_B|/M_A = \sqrt{\lambda}/2$, with $\lambda \equiv \lambda(1, z, r^2) = 1 + z^2 + r^4 - 2z - 2r^2 - 2zr^2$ the standard kinematical function and $r \equiv M_B/M_A$. Specifically,

$$\Gamma(A \rightarrow B\gamma\gamma) = \int_0^{(1-r)^2} dz \frac{d\Gamma}{dz}[z] = \int_0^{(1-r^2)/2} \frac{2P_B dP_B}{\sqrt{r^2 + P_B^2}} \frac{d\Gamma}{dz} \left[z(P_B) = 1 + r^2 - 2\sqrt{P_B^2 + r^2} \right]. \quad (1)$$

To match the observed ATLAS spectrum [1], all that is needed is a differential rate falling down sufficiently fast above 750 GeV. Far below the peak, the SM background quickly increases and would wipe out any sensitivity to the $A \rightarrow B\gamma\gamma$ process. Still, slightly below the peak, at around 600 GeV, the event rate matches the background. Even if this corresponds only to a few data point, for which the uncertainty is still rather large, the differential rate should preferably fall down not too slowly as $m_{\gamma\gamma}^2$ decreases.

2 Effective four-point interactions

To check whether a peaked behavior for the diphoton invariant mass spectrum is realistic, and since the nature of the decaying state is no longer constrained, we can consider various assignments for A and B . Our basic assumption is that A and B are neutral under the SM gauge group, but nevertheless share some conserved charge χ . If $\chi(A) = -\chi(B)$, the effective interactions involving a pair of photons can derive from either

$$\text{Scalar case : } \mathcal{L}_{eff} = \frac{1}{\Lambda^2} (S_A S_B F_{\mu\nu} F^{\mu\nu} + S_A S_B F_{\mu\nu} \tilde{F}^{\mu\nu}), \quad (2a)$$

$$\text{Fermion case : } \mathcal{L}_{eff} = \frac{1}{\Lambda^3} (\bar{\psi}_A^C \psi_B F_{\mu\nu} F^{\mu\nu} + \bar{\psi}_A^C \gamma_5 \psi_B F_{\mu\nu} \tilde{F}^{\mu\nu} + h.c.), \quad (2b)$$

$$\text{Vector case : } \mathcal{L}_{eff} = \frac{1}{\Lambda^4} (A_{\alpha\beta} B^{\alpha\beta} F_{\mu\nu} F^{\mu\nu} + A_{\alpha\beta} \tilde{B}^{\alpha\beta} F_{\mu\nu} \tilde{F}^{\mu\nu} + \dots), \quad (2c)$$

where $\tilde{F}^{\mu\nu} = \frac{1}{2} \varepsilon^{\mu\nu\rho\sigma} F_{\rho\sigma}$ and possible Wilson coefficients dressing each operator can be thought as being absorbed in the scale Λ for notation clarity. These effective operators are all independent, and assumed valid above the electroweak scale. In this respect, they should thus actually be written in terms of the $SU(2)_L$ and/or $U(1)_Y$ field strengths. For instance, replacing

$$F^{\mu\nu} \rightarrow B^{\mu\nu} = \cos \theta_W F^{\mu\nu} - \sin \theta_W Z^{\mu\nu}, \quad (3)$$

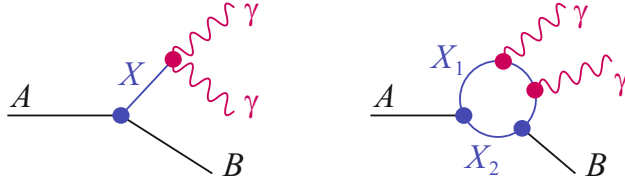


Figure 1: Example of short-distance processes leading to the effective interactions in Eq. (2). For the tree-level diagram, X is a scalar or tensor state, whose coupling to two photons must involve yet another state. For the loop diagram, there must be a pair of states circulating the loop to ensure χ conservation.

the $\gamma\gamma$, $Z\gamma$, and ZZ modes would be produced in the ratio $1 : 2 \tan^2 \theta_W : \tan^4 \theta_W$, up to kinematical effects (in exactly the same way as for the two-body interpretation of the diphoton anomaly, see *e.g.* Ref. [13]). Finally, the CP symmetry can be enforced without loss of generality, since it is always possible to set the two photons in the adequate CP state ($F_{\mu\nu}F^{\mu\nu}$ and $F_{\mu\nu}\tilde{F}^{\mu\nu}$ have opposite parity).

At this stage, the main issue is whether simpler interactions, as for instance those involving a single photon, are possible. Though a full answer to this question would require constructing full-fledged UV completions, which is well beyond our current scope, we can nevertheless draw a number of observations. These effective interactions could either arise at tree level or at loop level, see Fig. 1, and in general require more than one extra state. For instance, in the former case, the additional resonance X would be a scalar or tensor state coupled to two photons. We only allow it to be off-shell, since otherwise the three-body signature would be lost. The X would simply be a true diphoton resonance with a mass of 750 GeV. Still, even if off-shell, this state can couple to two photons only through additional new degrees of freedom, for example a vector fermion loop. The main interest of this scenario is that the single-photon processes are automatically absent.

If generated at loop level, two new states are also required in general to ensure the conservation of χ and prevent $A, B \rightarrow \gamma\gamma$. Both of them could be fermions when A and B are scalars or vectors, but at least one new scalar or vector is needed to induce $\psi_A \rightarrow \psi_B \gamma\gamma$. The only exception is the charged scalar loop when A, B are themselves also scalars, with a renormalizable ABX^+X^- vertex. Anyway, looking at Fig. 1, it seems obvious that such loops induce also single photon modes (along with potentially large mixings between the two states, which we assumed have been dealt with properly so that states occurring in the effective interactions are true mass eigenstates). Whether such processes truly occur, and in case they do, the relative strength of the one and two photon modes, depends on the nature of A and B , so we now discuss the various assignments separately.

Scalar transitions

The single photon production $S_A \rightarrow S_B \gamma$ is forbidden by Lorentz and gauge invariance (for the same reason as, *e.g.*, $K^+ \not\rightarrow \pi^+ \gamma$ or $\eta \not\rightarrow \pi^0 \gamma$). At the renormalizable level, trivially, a direct coupling of the photon field A^μ to the scalar current $S_A \partial_\mu S_B - S_B \partial_\mu S_A$ is not gauge invariant since the current is not conserved when $m_A \neq m_B$. Beyond leading order, effective operators involving a single photon field can be constructed, for instance

$$\frac{1}{\Lambda^2} S_A \partial^\nu S_B \partial^\mu F_{\mu\nu}, \quad (4)$$

but the amplitude necessarily vanishes for an on-shell photon. There is no corresponding operator involving $\tilde{F}^{\mu\nu}$, as can be easily understood at the Feynman rule level since there are only three

independent four-vectors to be contracted with $\varepsilon^{\mu\nu\rho\sigma}$. This implies that if S_A and S_B are real fields with the same parity, then $S_A \rightarrow S_B\gamma^*$ is CP-violating (as is *e.g.* $\eta \rightarrow \pi^0\ell^+\ell^-$).

Interestingly, this could suffice to reduce the $S_A \rightarrow S_B\ell^+\ell^-$ or $S_A \rightarrow S_Bq\bar{q}$ signals, even when CP conserving. Since the effective interaction is of the same dimension as the two-photon ones, producing the fermion pair through $A \rightarrow B[\gamma^* \rightarrow f\bar{f}]$ is at best comparable to the $\gamma\gamma$ mode, and could actually end up very suppressed if the situation for $K^0 \rightarrow \pi^0\gamma\gamma$ compared to $K_S \rightarrow \pi^0\ell^+\ell^-$ is of any guide [42].

Coming back to the vector fermion loop, it is easy to see that it never induces the operator Eq. (4). If both scalars couple as $S_{A,B}\bar{\psi}_F\psi_F$ or $S_{A,B}\bar{\psi}_F\gamma_5\psi_F$ with ψ_F the electrically charged heavy vector fermion circulating in the loop, then the process is CP-violating and the sum of the two diagrams where ψ_F circles clockwise and anticlockwise cancel each other. If one scalar couples through $\bar{\psi}_F\psi_F$ and the other through $\bar{\psi}_F\gamma_5\psi_F$, then both amplitudes are proportional to $\varepsilon_{\mu\nu\rho\sigma}(\varepsilon_\gamma^*)^\mu p_A^\nu p_B^\rho p_\gamma^\sigma = 0$ since $p_A = p_B + p_\gamma$. At this level, single photon processes cannot be induced.

Vector transitions

For the vector case, first remark that we do not consider all possible index contractions among the four field strengths in Eq. (2), but only some representative examples from the point of view of the differential rate. More importantly, we have not included dimension-six operators like $A_\alpha B^\alpha F_{\mu\nu} F^{\mu\nu}$ for three reasons. First, those would lead to differential rates very similar to the scalar case. Second, they may be quite complicated to generate from some UV completion. Finally, nothing would prevent a renormalizable coupling to a single photon like $A^\mu B^\nu F_{\mu\nu}$. The Landau-Yang theorem does not apply without gauge invariance or with two different vector bosons in the final state.

Even if we insist on constructing only operators involving field strengths, the $V_A \rightarrow V_B\gamma$ process is not manifestly forbidden because $m_{A,B} \neq 0$, as can be seen starting with

$$\frac{1}{\Lambda^2}(A_{\nu\alpha}B^{\alpha\mu}F_\mu^\nu + A_{\nu\alpha}B^{\alpha\mu}\tilde{F}_\mu^\nu + \dots). \quad (5)$$

Nevertheless, the $V_A \rightarrow V_B\gamma$ process along with $V_A \rightarrow V_B[\gamma^* \rightarrow \ell^+\ell^-, q\bar{q}]$ could be very suppressed. Taking again the vector fermion loop, and assuming V_A and V_B have both either vector or axial-vector couplings to ψ_F , charge conjugation ensures the cancellation of all the diagrams to which an odd number of vector fields are attached. So, instead of the Landau-Yang theorem, what really matters in this case is the Furry theorem of QED. Note that axial-vector couplings seem more tenable to prevent the kinetic mixing $V_{A,B} \leftrightarrow \gamma$, though we have not analyzed the vector coupling scenario further.

Fermion transitions

For the fermion case, operators involving a single field strength are not forbidden. Gauge invariance prevents the direct coupling to the fermion current $\bar{\psi}_A^C\gamma_\mu\psi_B$, but one can construct

$$\frac{1}{\Lambda}(\bar{\psi}_A^C\sigma_{\mu\nu}\psi_B F^{\mu\nu} + \bar{\psi}_A^C\sigma_{\mu\nu}\psi_B \tilde{F}^{\mu\nu}). \quad (6)$$

Contrary to the scalar case, these operators produce an on-shell photon, are of lower dimension than those in Eq. (2), and both $F^{\mu\nu}$ and $\tilde{F}^{\mu\nu}$ can occur so CP can be of no help. If arising at loop level, there does not seem to be any obvious way to enhance the two-photon relative to the one-photon emission (besides asking for ψ_B to decay rather quickly into a photon plus yet another fermion ψ_C). Phenomenologically, the fermionic scenario is most likely to make sense only in the tree-level hypothesis.

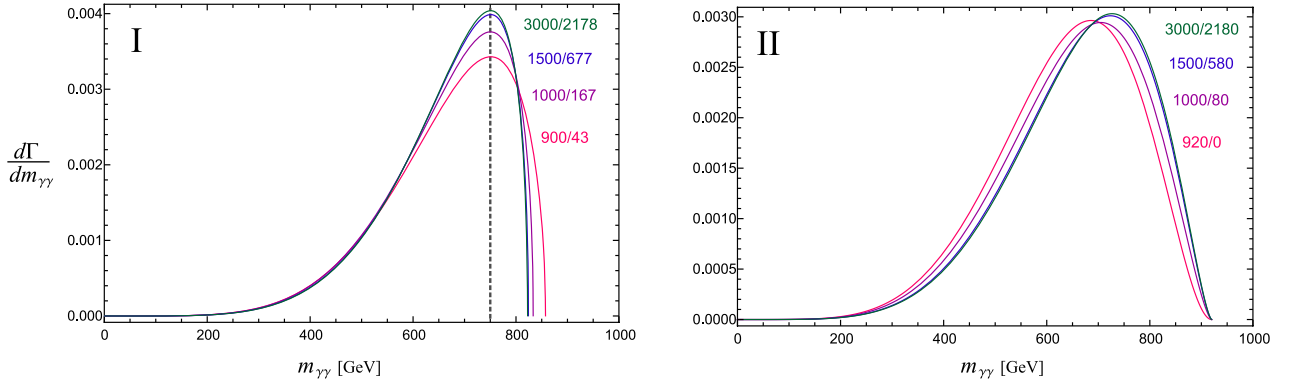


Figure 2: No matter the effective operator, differential diphoton spectra fall in one of two classes: those peaking at high diphoton invariant mass (left panel), and those peaking closer to the average diphoton mass (right panel). Specifically, all but the $\psi_A \gamma_5 \psi_B F_{\mu\nu} \tilde{F}^{\mu\nu}$ and $A_{\alpha\beta} \tilde{B}^{\alpha\beta} F_{\mu\nu} \tilde{F}^{\mu\nu}$ are in the first class. Therefore, in the left panel, we show the differential rate for the scalar case for various choices of M_A , and with M_B fixed (the labels close to each curve denote M_A/M_B , in GeV) so that the peak is precisely at 750 GeV.

3 Differential rates and interpretation

The differential rates are straightforward to compute for these various cases, giving

$$\frac{d\Gamma}{dz}(S_A \rightarrow S_B \gamma\gamma)_{+-,-+} = \frac{M_A^5}{32\pi^3 \Lambda^4} z^2 \lambda(1, z, r^2)^{1/2}, \quad (7a)$$

$$\frac{d\Gamma}{dz}(\psi_A \rightarrow \psi_B \gamma\gamma)_{++} = \frac{M_A^7}{64\pi^3 \Lambda^6} z^2 \lambda(1, z, r^2)^{1/2} ((r+1)^2 - z), \quad (7b)$$

$$\frac{d\Gamma}{dz}(\psi_A \rightarrow \psi_B \gamma\gamma)_{-+} = \frac{M_A^7}{16\pi^3 \Lambda^6} z^2 \lambda(1, z, r^2)^{1/2} ((r-1)^2 - z), \quad (7c)$$

$$\frac{d\Gamma}{dz}(V_A \rightarrow V_B \gamma\gamma)_{++} = \frac{M_A^9}{4\pi^3 \Lambda^8} z^2 \lambda(1, z, r^2)^{1/2} (6r^2 + \lambda(1, z, r^2)), \quad (7d)$$

$$\frac{d\Gamma}{dz}(V_A \rightarrow V_B \gamma\gamma)_{-+} = \frac{M_A^9}{4\pi^3 \Lambda^8} z^2 \lambda(1, z, r^2)^{3/2}, \quad (7e)$$

where the subscripts denote a scalar (++) or pseudoscalar (-+) coupling to $F_{\mu\nu} F^{\mu\nu}$ or $F_{\mu\nu} \tilde{F}^{\mu\nu}$, respectively. From these shapes, we can draw a number of conclusions:

1. All the differential rates show a strong dependence on $m_{\gamma\gamma}$, which can be traced to the photon momenta arising from the derivatives present in $F_{\mu\nu} F^{\mu\nu}$ or $F_{\mu\nu} \tilde{F}^{\mu\nu}$. More generally and model-independently, Low's theorem [3] tells us that when A and B are electrically neutral, the $A \rightarrow B \gamma\gamma$ amplitude must be at least linear in the photon energy E_γ as $E_\gamma \rightarrow 0$. At larger $m_{\gamma\gamma}$, the squared amplitude is dampened by the kinematical factors forcing $d\Gamma/dm_{\gamma\gamma}$ to go back to zero at the high-energy end-point. In the middle, the differential rate thus always shows a peak. Interestingly, requiring it to be close to its high-energy end-point does not suffice to discriminate between spin 0, 1/2, or 1 resonances. All we can say asking for a high $m_{\gamma\gamma}^2$ peak is that a few couplings cannot match the observed anomaly, with $\bar{\psi}_A^C \gamma_5 \psi_B F_{\mu\nu} \tilde{F}^{\mu\nu}$ and $A_{\alpha\beta} \tilde{B}^{\alpha\beta} F_{\mu\nu} \tilde{F}^{\mu\nu}$ producing only a broad bump in the middle of the kinematical range, see

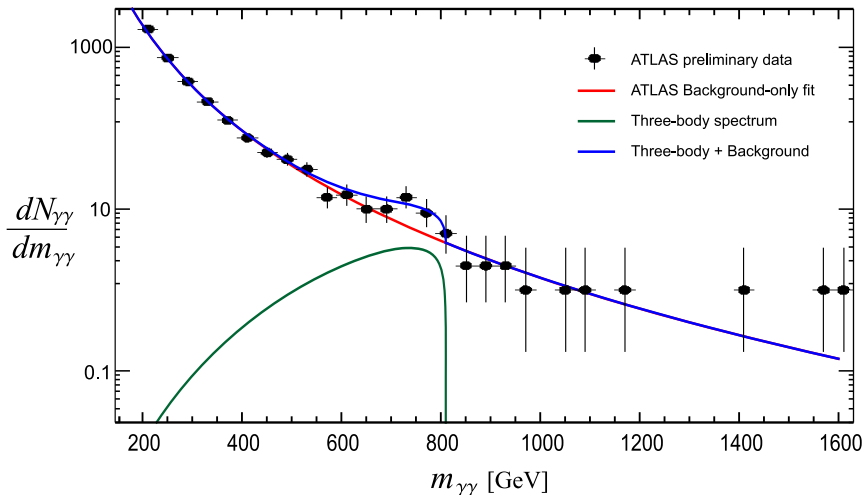


Figure 3: Impact of a three-body production of a pair of photons, for $M_A = 1.5$ TeV and $M_A - M_B = 810$ GeV, over the background observed by ATLAS [1]. Lacking all the details about the data points, their errors, and correlations, the $A \rightarrow B\gamma\gamma$ rate is adjusted by hand.

Fig. 2. On the other hand, for all the other operators, the spectrum is very similar and peaks at high diphoton invariant mass. Its shape is quite consistent with the observed events, see Fig. 3. In this respect, note how the peak initially gets more pronounced as M_A increases, but quickly reaches a limiting shape and does not change significantly beyond $M_A \approx 1.5$ TeV.

2. The mass scale of the process is always higher than 750 GeV, because for $m_{\gamma\gamma}$ to peak there, the mass of the decaying resonance has to be above about 900 GeV. Actually, it is even possible for the A resonance to be well above the TeV scale. This automatically helps explaining why no such signal was seen at 8 TeV. Indeed, the gain factor in cross section going from 8 TeV to 13 TeV, for a typical partonic production, increases with the resonance mass. For example, if produced through the gluon-gluon channel, the gain factor is of about 5.3 for $M_A = 900$ GeV, and already nearly twice as large, 9.3, for $M_A = 1.5$ TeV. Note, finally, that this also helps to pass the bounds obtained at 8 TeV in the γZ [47] and ZZ [48] channels.
3. If not forbidden (see previous section), this peaked behavior of the differential rate is not necessarily matched by single photon emission. For example, starting with the operator in Eq. (4) and coupling the virtual photon to a Dalitz pair, we find

$$\frac{d\Gamma}{dz}(S_A \rightarrow S_B[\gamma^* \rightarrow f\bar{f}]) = \frac{M_A^5}{256\pi^3\Lambda^4} \lambda(1, z, r^2)^{3/2}, \quad (8)$$

in the limit $m_f \rightarrow 0$, where $z = m_{\ell\ell}^2/M_A^2$ is now the reduced dilepton invariant mass. In this case, the photon momentum dependence of the effective vertex Eq. (4) is compensated by the $1/m_{\ell\ell}^2$ coming from the virtual photon propagator, and the differential rate ends up maximal at $z = 0$, falling off roughly linearly towards zero as $z \rightarrow (1-r)^2$. With such a shape devoid of any particular feature, and with the rather suppressed rate, the 8 TeV bounds are easily satisfied [46] and it is not even clear such a signal could be easily evidenced in the future.

4. Thanks to the strong peak at high $m_{\gamma\gamma}^2$, the invisible state escaping the detector would carry away a moderate amount of missing energy, as shown in Fig. 4. Typically, the B momentum

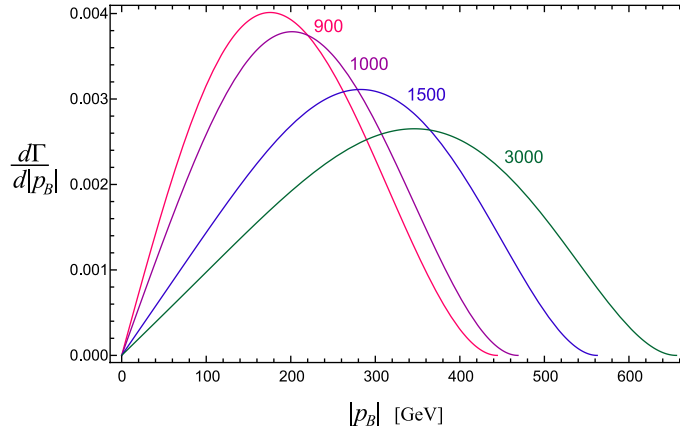


Figure 4: Spectrum of the B momentum in the A rest-frame for various M_A hypotheses. The effective $S_A S_B F_{\mu\nu} F^{\mu\nu}$ operator is chosen for definiteness.

in the A rest-frame peaks at about 15 – 20% of M_A . For example, with $M_A = 1.5$ TeV, it is maximum for $|\mathbf{p}_B| \approx 280$ GeV. Still, together with observing an excess in $\gamma\gamma$ events for lower invariant mass, it could help identify the three body nature of the process. Alternatively, but at the cost of allowing for the new charge χ to be violated at some point, the B particle could also decay, for example into a pair of rather soft photons or leptons which would have been cut away in selecting the $\gamma\gamma$ candidate events. Provided this state can only be produced via the decay of A , it could well have escape detection up to now.

- Finally, one could think of pushing the reasoning one step further and consider four-body decays $A \rightarrow B + C + \gamma\gamma$. As for the three-body processes, the momentum dependence hidden in the $F_{\mu\nu} F^{\mu\nu}$ or $F_{\mu\nu} \tilde{F}^{\mu\nu}$ structures still favors the presence of a peak for rather large diphoton invariant mass. On the other hand, a four-body interpretation has several short-comings. It is less trivial to design a single conserved charge able to prevent simpler cascade decays, or involving only one photon. In addition, the dimension of the effective operators are larger and the rate further phase-space suppressed, so Λ has to be systematically lower casting serious doubts on the effective treatment. Moreover, the missing energy carried away by both B and C could be too large to have stayed unnoticed.

4 On the scale of the effective operators

To explain the rather large observed $\gamma\gamma$ anomaly, the decay width into two photons and the production of the A resonance have to be sufficiently large. Up to now we did not consider the latter production, since our goal is to show the compatibility of the three-body hypothesis with the shape of the diphoton anomaly. Also, dealing with both production and decay is necessarily more model-dependent. So in this section, we will present a few arguments and, staying as generic as possible, give some estimates of the scale of the effective interactions.

As a first handle, we consider the scalar case with the production mechanism $gg \rightarrow S_A$:

$$\mathcal{L}_{eff} = \frac{\kappa_{gg}}{\Lambda} S_A G_{\mu\nu} G^{\mu\nu} + \frac{\kappa_{\gamma\gamma}}{\Lambda^2} S_A S_B F_{\mu\nu} F^{\mu\nu}. \quad (9)$$

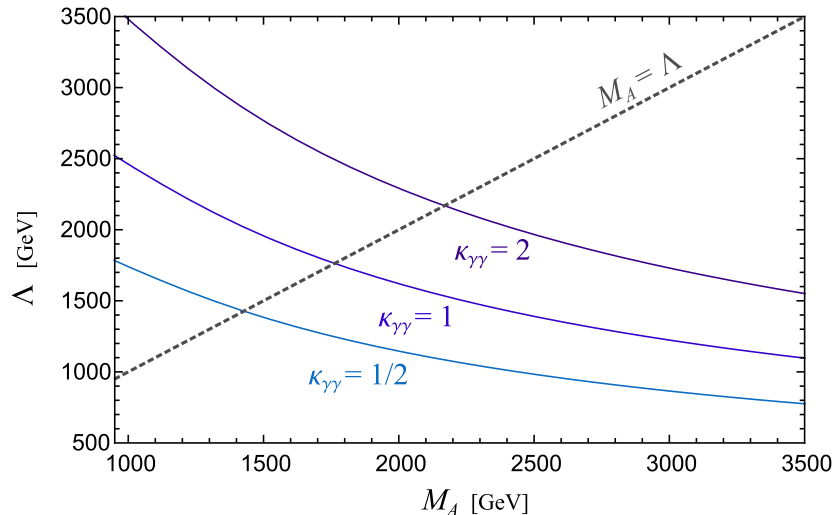


Figure 5: Scale Λ as a function of M_A , setting $\kappa_{\gamma\gamma} = 1/2, 1, 2$, required to reproduce the observed diphoton production rate. For simplicity, following Ref. [13], we assume for this plot that the electromagnetic width is sub-leading compared to the gg channel and neglect the evolution of the partonic gg density as a function of M_A , so as to fix $\Gamma(A \rightarrow B\gamma\gamma)/M_A \approx 1.1 \times 10^{-6}$.

Although the single production of S_A violates the charge χ , it is instructive to determine the evolution of Λ as a function of M_A in this simple scenario (a more realistic model will be discussed below), this is shown in Fig. 5. At this stage, the three-body scenario does not really help to explain the largeness of the $\gamma\gamma$ production rate required to match the observed anomaly, and actually fares worse than the two body scenario because of the extra phase-space suppression, and of the higher dimensionality of the operators. For the fermionic and vector cases, the higher dimension of the operators forces Λ to be lower.

To improve the situation, and provide one realistic setting in which the three body scenario would drive the diphoton anomaly, let us reconsider the decay and production.

Nearly resonant decay

As a first step, in view of the proximity of Λ and $M_A - M_B$, it is reasonable to expect that the underlying dynamics could be felt. Consider for instance the exchange of an off-shell scalar X , see Fig. 1. Its impact is to replace two powers of the scale Λ by

$$\frac{1}{\Lambda^2} \rightarrow \frac{-1}{m_{\gamma\gamma}^2 - M_X^2 + iM_X\Gamma_X}, \quad (10)$$

in the effective interactions of Eq. (2). The scale factor remaining after this substitution then concerns only the $X\gamma\gamma$ and XAB couplings (the former has mass dimension -1 , while the latter has mass dimension $1, 0$, and -1 when A, B are scalars, fermions, or vectors, respectively). Clearly, when M_X is only barely larger than $M_A - M_B$, the slightly off-shell X propagator strengthens the peak of the differential rate at high $m_{\gamma\gamma}^2$. Further, simply for dimensional reasons, the constraints on the scale Λ tuning the $X \rightarrow \gamma\gamma$ vertex are then much weaker, and tend towards those typical of the two-photon resonance scenario (see *e.g.* Ref. [13]). More generally, such a conclusion can be reached whenever

a form-factor $F(m_{\gamma\gamma}^2)$, whose typical expansion would be $F(m_{\gamma\gamma}^2) = 1 + \alpha m_{\gamma\gamma}^2/M_A^2 + \mathcal{O}(m_{\gamma\gamma}^4/M_A^4)$, needs to be inserted to account for the short-distance dynamics. With $\alpha > 0$, such a form-factor further strengtens the peak of the differential rate at high $m_{\gamma\gamma}^2$.

Production of the parent resonance

Given our hypothesis of a new conserved quantum number for the A and B particles, it would be more adequate to consider the $gg \rightarrow A + B$ process. There is indeed no obstruction to replace the photon by the gluon field strength in the effective operators. In that case, $A \rightarrow B\gamma\gamma$ would be accompanied by $A \rightarrow Bgg$. The dijet invariant mass would follow the same distribution as the two-photon one, and would thus peak again around 750 GeV. Note, however, that the decay rate $A \rightarrow Bgg$ and the production mechanism $gg \rightarrow A + B$ are far less easy to relate than $gg \rightarrow A$ and $A \rightarrow gg$ in the two-body hypothesis. The typical scale of the $gg \rightarrow A + B$ process is higher than M_A since the gluons must carry at least an energy equal to $M_A + M_B$ in their center of mass. Furthermore, since the scale Λ cannot be much higher than M_A , the structure of the effective $ggAB$ vertex is likely to become very relevant for production. It could even begin to resonate if we imagine that these vertices arise from tree-level or loop processes, in which case a cascade decay mechanism would need to be considered. This means that in principle, the $gg \rightarrow A + B$ production could be quite strong even with a moderate dijet production $A \rightarrow Bgg$, in agreement with the current absence of a signal in the latter.

To make this statement more precise we should give up our model-independent formalism. So, for illustration, let us consider a scenario in which both the effective $A \rightarrow Bgg$ and $A \rightarrow B\gamma\gamma$ decays are induced by the exchange of an off-shell scalar X , with A and B either scalars, fermions, or vectors. Then, the production of the A particle can proceed via an on-shell X , so that in the narrow width approximation,

$$\sigma(pp \rightarrow \gamma\gamma BB) = \frac{C_{gg}(M_X)}{M_X s} \Gamma(X \rightarrow gg) \frac{1}{\Gamma_X} \Gamma(X \rightarrow AB) \frac{1}{\Gamma_A} \Gamma(A \rightarrow B\gamma\gamma) , \quad (11)$$

where $C_{gg}(M_X)$ is the gg partonic integral for a resonance of mass M_X at the $\sqrt{s} = 13$ TeV LHC. We evaluated $C_{gg}(M_X)$ at a scale $\mu_F = M_X$ using the NNPDF 3.0 parton distribution functions [49],

M_X [TeV]	0.9	1.0	1.5	2.0	3.0
$C_{gg}(M_X)$	863	491	47	7	0.3

(12)

Assuming that $\text{BR}(X \rightarrow AB) \approx 1$ and setting $\sigma(pp \rightarrow \gamma\gamma BB) \approx 6$ fb [19], this simplifies to

$$\frac{\Gamma(X \rightarrow gg)}{M_X} \text{BR}(A \rightarrow B\gamma\gamma) = \frac{s\sigma(pp \rightarrow \gamma\gamma BB)}{C_{gg}(M_X)} \approx \frac{2.5 \times 10^{-3}}{C_{gg}(M_X)} . \quad (13)$$

Thus, even though $C_{gg}(M_X)$ quickly decreases with increasing M_X , this does not imply that $\Gamma(A \rightarrow B\gamma\gamma)$ should also increase. If $A \rightarrow B\gamma\gamma$ and $A \rightarrow Bgg$ are the only two available decay modes, then all is needed is a non-suppressed $\text{BR}(A \rightarrow B\gamma\gamma)$. Small $\text{BR}(A \rightarrow Bgg)$ is also preferable in order to suppress the potential di-jet signature. Taking for definiteness $\text{BR}(A \rightarrow B\gamma\gamma) = 1/2$, the effective scale is only constrained by the initial X production:

$$\frac{5 \times 10^{-3}}{C_{gg}(M_X)} \approx \frac{\Gamma(X \rightarrow gg)}{M_X} = 8\pi\alpha_3^2 \frac{M_X^2}{\Lambda_X^2} , \quad (14)$$

where in the last equality we assumed an effective coupling $(g_3^2/\Lambda_X)XG_{\mu\nu}G^{\mu\nu}$. Such small rates actually push the scale to very high values,

$$\frac{M_X [\text{TeV}]}{\Lambda_X [\text{TeV}]} \left| \begin{array}{ccccc} 0.9 & 1.0 & 1.5 & 2.0 & 3.0 \\ \hline 184 & 154 & 72 & 38 & 12 \end{array} \right. \quad (15)$$

Note that this does not imply too long lifetimes for the A particle, since the scale Λ_X only tunes the $X\gamma\gamma$ and Xgg couplings (in other words, remember that in Eq. (7), four powers of Λ should be replaced by M_X^4 , see Eq. (10)).

Finally, it is instructive to compare this interpretation with the two-body scenario. If X is directly responsible for the diphoton anomaly, we can write

$$\sigma(pp \rightarrow \gamma\gamma, jj) = \frac{C_{gg}(M_X)}{s} \frac{\Gamma(X \rightarrow gg)\Gamma(X \rightarrow \gamma\gamma, gg)}{M_X\Gamma_X}. \quad (16)$$

Then, assuming $\Gamma(X \rightarrow gg) \ll \Gamma_X \approx \Gamma(X \rightarrow \gamma\gamma)$, the scale derived from $X \rightarrow gg$ are consistent with those quoted above. However, reproducing the diphoton production rate forces $\Gamma(X \rightarrow \gamma\gamma)$ to be very large. Assuming an interaction of the form $(e^2/\Lambda_\gamma)XF_{\mu\nu}F^{\mu\nu}$, its effective scale has to be dangerously lower than Λ_X (see Fig. 1 in Ref. [13]). In the three-body scenario on the contrary, both $\Gamma(X \rightarrow gg) \approx \Gamma(X \rightarrow \gamma\gamma) \ll \Gamma_X$ can be tiny because the large diphoton rate is ensured thanks to the large $\text{BR}(X \rightarrow AB)$ and $\text{BR}(A \rightarrow B\gamma\gamma)$. This is certainly consistent with the dimensions of the interactions: Xgg and $X\gamma\gamma$ are necessarily suppressed by some high scale Λ_X , but the ABX vertex could even be renormalizable when A, B are scalars or fermions. Thus, in the present scenario, the diphoton signal overwhelmingly arises from the three-body decay of the A particle, while the $gg \rightarrow X \rightarrow \gamma\gamma, gg$ remains tiny.

5 Concluding remarks

Theoretically, interpreting the anomaly observed in the two-photon invariant mass spectrum as arising from a three-body process $A \rightarrow B\gamma\gamma$ has two main advantages. There is no need to account for a large width for the parent particle, and it is quite natural for the involved new particles to share some conserved quantum numbers. This should be welcome for many models where such charges are introduced, *e.g.*, to ensure the stability of a light DM candidate or a suppression of FCNC (as R-parity in supersymmetry). On the other hand, the main disadvantage of this scenario is the higher dimensionality of the effective interactions. If taken seriously, the diphoton anomaly is surprisingly large, and is already non-trivial to reproduce in the two-body decay scenario. With three bodies, the situation seems to worsen with the effective interaction scale ending up even lower. While this is generically true, the three-body nature of the process opens new alternative production mechanisms and there are ways to circumvent this problem. We have provided one such example, in which the $AB\gamma\gamma$ and $ABgg$ interactions arise from the exchange of a scalar resonance X . In that case, the scale of the New Physics inducing both the $X\gamma\gamma$ and Xgg vertices could still be far above the TeV. This is actually an improvement over the pure 750 GeV diphoton resonance scenario, in which the scale of at least one of these vertices has to be close to the TeV, see *e.g.* Ref. [13].

Experimentally, discriminating this scenario from a pure two-photon resonance would of course be achieved with a better resolution of $d\Gamma(pp \rightarrow \gamma\gamma)/dm_{\gamma\gamma}^2$, especially below the 750 GeV peak. Even if modulated by some effective form factor, the shape of the differential rate should significantly depart from the simple Breit-Wigner expected for a diphoton resonance. On the other hand, we find that the

shape of the differential rate does not constrain the spin of the A, B particles, with scalars, fermions, or vectors producing essentially the same signature.

To further confirm the three-body nature of the process, the presence of some missing energy could be a tell-tale sign since the daughter particle B in $A \rightarrow B\gamma\gamma$ is never strictly at rest (the differential rate vanishes at the end-points). For the same reason, the two photons are never flying precisely back-to-back in the A rest frame, so their angular distribution could provide complementary information. Note in addition that missing energy may arise if B particle also accompany the production of the A particle, like in a $gg \rightarrow B + [A \rightarrow B\gamma\gamma]$ chain.

On the other hand, $Z\gamma$ and ZZ signals, which should be seen at some point, would not help pinpoint the nature of the process since they should occur in the same ratios respective to $\gamma\gamma$ as in the two-body decay scenario. Similarly, some peak in the dijet spectrum would seem likely but would not be characteristic. Note however that this depends on the true production mechanism for the parent particle, which could proceed instead through some cascades from other yet unknown particles. Finally, lepton pairs or quark pairs would be generically suppressed in this scenario, and no signal should be seen there.

Acknowledgments

We are grateful to Sabine Kraml for numerous discussions. This work has been supported in part by the “Investissements d’avenir, Labex ENIGMASS”.

References

- [1] ATLAS 13 TeV Results - December 2015. Talk by Marumi Kado at CERN, and ATLAS note: ATLAS-CONF-2015-081.
- [2] CMS 13 TeV Results - December 2015. Talk by Jim Olsen at CERN, and CMS note: CMS-PAS-EXO-15-004.
- [3] F. E. Low, Phys. Rev. **110** (1958) 974. doi:10.1103/PhysRev.110.974
- [4] K. Harigaya and Y. Nomura, [arXiv:1512.04850](#) [hep-ph].
- [5] Y. Mambrini, G. Arcadi and A. Djouadi, [arXiv:1512.04913](#) [hep-ph].
- [6] M. Backovic, A. Mariotti and D. Redigolo, [arXiv:1512.04917](#) [hep-ph].
- [7] A. Angelescu, A. Djouadi and G. Moreau, [arXiv:1512.04921](#) [hep-ph].
- [8] Y. Nakai, R. Sato and K. Tobioka, [arXiv:1512.04924](#) [hep-ph].
- [9] S. Knapen, T. Melia, M. Papucci and K. Zurek, [arXiv:1512.04928](#) [hep-ph].
- [10] S. Di Chiara, L. Marzola and M. Raidal, [arXiv:1512.04939](#) [hep-ph].
- [11] A. Pilaftsis, [arXiv:1512.04931](#) [hep-ph].
- [12] D. Buttazzo, A. Greljo and D. Marzocca, [arXiv:1512.04929](#) [hep-ph].
- [13] R. Franceschini *et al.*, [arXiv:1512.04933](#) [hep-ph].

- [14] E. Molinaro, F. Sannino and N. Vignaroli, [arXiv:1512.05334](#) [hep-ph].
- [15] C. Petersson and R. Torre, [arXiv:1512.05333](#) [hep-ph].
- [16] R. S. Gupta, S. Jäger, Y. Kats, G. Perez and E. Stamou, [arXiv:1512.05332](#) [hep-ph].
- [17] B. Bellazzini, R. Franceschini, F. Sala and J. Serra, [arXiv:1512.05330](#) [hep-ph].
- [18] M. Low, A. Tesi and L. T. Wang, [arXiv:1512.05328](#) [hep-ph].
- [19] J. Ellis, S. A. R. Ellis, J. Quevillon, V. Sanz and T. You, [arXiv:1512.05327](#) [hep-ph].
- [20] S. D. McDermott, P. Meade and H. Ramani, [arXiv:1512.05326](#) [hep-ph].
- [21] T. Higaki, K. S. Jeong, N. Kitajima and F. Takahashi, [arXiv:1512.05295](#) [hep-ph].
- [22] B. Dutta, Y. Gao, T. Ghosh, I. Gogoladze and T. Li, [arXiv:1512.05439](#) [hep-ph].
- [23] Q. H. Cao, Y. Liu, K. P. Xie, B. Yan and D. M. Zhang, [arXiv:1512.05542](#) [hep-ph].
- [24] Y. Bai, J. Berger and R. Lu, [arXiv:1512.05779](#) [hep-ph].
- [25] D. Aloni, K. Blum, A. Dery, A. Efrati and Y. Nir, [arXiv:1512.05778](#) [hep-ph].
- [26] A. Falkowski, O. Slone and T. Volansky, [arXiv:1512.05777](#) [hep-ph].
- [27] C. Csaki, J. Hubisz and J. Terning, [arXiv:1512.05776](#) [hep-ph].
- [28] A. Ahmed, B. M. Dillon, B. Grzadkowski, J. F. Gunion and Y. Jiang, [arXiv:1512.05771](#) [hep-ph].
- [29] P. Agrawal, J. Fan, B. Heidenreich, M. Reece and M. Strassler, [arXiv:1512.05775](#) [hep-ph].
- [30] J. Chakraborty, A. Choudhury, P. Ghosh, S. Mondal and T. Srivastava, [arXiv:1512.05767](#) [hep-ph].
- [31] L. Bian, N. Chen, D. Liu and J. Shu, [arXiv:1512.05759](#) [hep-ph].
- [32] D. Curtin and C. B. Verhaaren, [arXiv:1512.05753](#) [hep-ph].
- [33] S. Fichtel, G. von Gersdorff and C. Royon, [arXiv:1512.05751](#) [hep-ph].
- [34] W. Chao, R. Huo and J. H. Yu, [arXiv:1512.05738](#) [hep-ph].
- [35] S. V. Demidov and D. S. Gorbunov, [arXiv:1512.05723](#) [hep-ph].
- [36] J. M. No, V. Sanz and J. Setford, [arXiv:1512.05700](#) [hep-ph].
- [37] D. Becirevic, E. Bertuzzo, O. Sumensari and R. Z. Funchal, [arXiv:1512.05623](#) [hep-ph].
- [38] P. Cox, A. D. Medina, T. S. Ray and A. Spray, [arXiv:1512.05618](#) [hep-ph].
- [39] R. Martinez, F. Ochoa and C. F. Sierra, [arXiv:1512.05617](#) [hep-ph].
- [40] A. Kobakhidze, F. Wang, L. Wu, J. M. Yang and M. Zhang, [arXiv:1512.05585](#) [hep-ph].
- [41] S. Matsuzaki and K. Yamawaki, [arXiv:1512.05564](#) [hep-ph].

- [42] K. A. Olive et al. [Particle Data Group Collaboration], Chin. Phys. C **38** (2014) 090001.
- [43] CMS Collaboration, CMS-PAS-EXO-14-005.
- [44] G. Aad *et al.* [ATLAS Collaboration], Phys. Rev. D **91** (2015) 052007.
- [45] V. Khachatryan *et al.* [CMS Collaboration], [arXiv:1512.01224](#) [hep-ex].
- [46] G. Aad *et al.* [ATLAS Collaboration], Phys. Rev. D **90** (2014) 5, 052005 [[arXiv:1405.4123](#) [hep-ex]].
- [47] G. Aad *et al.* [ATLAS Collaboration], Phys. Lett. B **738** (2014) 428 [[arXiv:1407.8150](#) [hep-ex]].
- [48] G. Aad *et al.* [ATLAS Collaboration], Eur. Phys. J. C **76** (2016) 1, 45 [[arXiv:1507.05930](#) [hep-ex]].
- [49] R. D. Ball *et al.* [NNPDF Collaboration], JHEP **1504**, 040 (2015) doi:10.1007/JHEP04(2015)040